

Key words: supernovae: general - methods: statistical - techniques: spectroscopic

An investigation on the FWHM of absorption features of type Ia supernovae

Xulin Zhao^{1,*}, Keiichi Maeda² and Xiaofeng Wang^{3,*}

¹ Tianjin Key Laboratory of Quantum Optics and Intelligent Photonics, School of Science, Tianjin University of Technology, Tianjin 300384, China

² Department of Astronomy, Kyoto University, Kyoto, 606-8502, Japan

³ Department of Physics, Tsinghua University, Beijing, 100084, China

Received 202x month day; accepted 202x month day

Abstract We present an investigation of the full width at half maximum (FWHM, or γ) of absorption features of Type Ia supernova (SNe Ia). We found that, the average value of FWHM can be well predicted with the rest wavelength (λ). The velocity also plays an important role, as objects with a higher velocity tend to have a larger FWHM. Temperature may be the third factor, as we found that, at the same velocity (but different phases), a normal-velocity (NV) object tends to have a larger FWHM than high-velocity (HV) object. Also, 1991T/1999aa-like objects that are believed to have relatively high temperatures show the largest FWHMs if compared at the same velocity. Generally speaking, FWHM evolves very slowly with time and shows no correlation with Δm_{15} , but 1991T/1999aa-like objects are characterized by relatively fast decreasing FWHM. On the other hand, we found that, objects with relatively small FWHMs shows a tighter correlation between absorption depth (A) and Δm_{15} , possibly a sign of higher degree of homogeneity. We also found that A/γ of Si II $\lambda 5972$ has a strong correlation with Δm_{15} , and more importantly, a relatively slow time evolution, making it a useful luminosity estimator even in the absence of phase information.

1 INTRODUCTION

Type Ia supernovae (SNe Ia) serve as a critical measurement tool in cosmology, with extremely bright and well standardable luminosity (e.g. Phillips 1993; Phillips et al. 1999; Riess et al. 1998, 2019; Perlmutter et al. 1999; Freedman et al. 2019; Jha et al. 2019). Physically, SNe Ia are caused by rapid thermonuclear runaway explosion. This usually happens when the white dwarf's mass approached the Chandrasekhar limit ($\approx 1.4M_{\odot}$), and then electron's degeneracy pressure was not able to counteract the gravitational force (e.g. Nomoto 1982; Khokhlov 1991; Hillebrandt & Niemeyer 2000; Maeda et al. 2010, 2018; Flörs et al. 2020). However, the conditions of explosion are not absolutely strict. For example, sub-Chandrasekhar mass explosion could be possible (e.g. Kushnir et al. 2013; Pakmor et al. 2013;

* zhaoxulin@139.com, <https://orcid.org/0000-0002-3204-2358>

* wang_xf@mail.tsinghua.edu.cn

Blondin et al. 2018; Shen et al. 2018; Flörs et al. 2020). Progenitor system could be different too: (1) Single degenerate scenario (SD): The progenitor could be a CO white dwarf which accreted mass from a non-degenerate companion star (such as a main-sequence or red-giant star, e.g. Whelan & Iben 1973; Nomoto 1982; Ruiz-Lapuente et al. 2023). (2) Double degenerate scenario (DD): Namely composing two white dwarfs (e.g. Iben & Tutukov 1984; Webbink 1984). A possible event is the famous nearby supernova SN 2011fe. Observations suggested no companion star or dimer than a few percent of the sun (e.g. Li et al. 2011).

Due to uncertainties in initial condition, such as those we mentioned above, SN Ia actually has significant intrinsic diversities, and it restricts the accuracy of standardized luminosity. To reduce the deviations, people are looking for spectral indicators that are sensitive to the intrinsic diversity. For example, the velocity of Si II $\lambda 6355$ was found to be very helpful in extinction correction for the peak luminosity (Wang et al. 2009). Currently the tightest correlation between spectral and photometric indicators is found to be that of absorption depth (i.e. maximum absorption rate) of Si II $\lambda 5972$ (A^{Si5}) and decline rate Δm_{15} (see for example, Zhao et al. 2021). But it is still unclear whether this correlation may help improve the calibration of luminosity. An easier method is to restrict the sample to subclass. A convenient classification scheme was proposed by Wang et al. (2009). In this scheme, most objects are included in a ‘high velocity’ (HV) subclass which has a velocity of Si II $\lambda 6355$ (V^{Si6}) greater than 12,000 km/s at maximum light, and a ‘normal velocity’ (NV) subclass which has $V^{Si6} \leq 12,000$ km/s at maximum light. Other subclasses include 1991T-like (Filippenko et al. 1992b; Phillips 1992), 1999aa-like (Li et al. 2001), 1991bg-like (Filippenko et al. 1992a). Type 1991bg-like SNe Ia, on the contrary, undergo a less complete burning (a proof is their low luminosity), leaving more IMEs unburnt in the ejecta, and thus have stronger absorption lines. Type 1991T-like SNe Ia are characterized by weak lines of intermediate-mass elements, as a result of more complete burning. Type 1999aa-like objects have high luminosity but also relatively normal Si II $\lambda 6355$ feature. In practice, 1991T-like and 1999aa-like objects are often grouped together as 1991T/1999aa-like objects. The reason is that they are overall similar (main difference is in line strength) with bright luminosity, and also because their samples are often too small (see, e.g. Zhao et al. 2021). In Benetti’s scheme (Benetti et al. 2005), SNe Ia are divided into ‘Faint’, ‘high-velocity gradient (HVG)’, and ‘low-velocity gradient (LVG)’ subtypes. In Branch’s scheme (Branch et al. 2006, 2009), SNe Ia are divided into ‘core-normal (CN)’, ‘broad-lined (BL)’, ‘cool’, and ‘shallow silicon (SS)’.

The absorption strength of an absorption feature is determined by the absorption depth and the full width at half maximum (FWHM). The former represents the absorption rate at the central velocity, while the latter describes how fast the absorption rate decreases at the broadened velocities. The sum of absorption rates gives the ‘pseudo-equivalent width’ (pEW) which quantifies the total absorption strength. Compared with the absorption depth and the pseudo-equivalent width, the full width at half maximum is relatively unexplored. But, a better determination of this parameter can significantly improve spectral fittings. Also, its distributions could be useful in researches on the intrinsic diversity, or help constrain the parameters of the explosion models of SNe Ia. Also note that, the absorption feature may include an extra component called ‘high-velocity feature’ (HVF, e.g. Childress et al. 2014; Maguire et al. 2014; Silverman et al. 2015; Zhao et al. 2015; Meng et al. 2019; Ni et al. 2023; Hakobyan et al. 2025) component. These HVFs are

believed to be formed in outer layers, where the ejecta's velocities are higher than the photosphere. Their origins are still a mystery. But, evidences have been found, suggesting possible element transitions (e.g. oxygen to silicon, see for example Zhao et al. 2016) and matter transfer from inner shells to outer shells (see for example Zhao et al. 2024).

2 DATA AND MEASUREMENT

This work targets at regulations of the FWHM of absorption features of SNe Ia. Since the study is relatively general, no special restrictions were imposed on the sample. The spectra were primarily from the CfA supernova program (Matheson et al. 2008; Blondin et al. 2012), the Berkeley supernova program (Silverman et al. 2012a,b), Carnegie supernova project (CSP, Folatelli et al. 2013), and our own database. Also noted that, in this work, the measurements involved only photospheric components, no HVF component.

FWHM is defined as the width of a curve at half of the maximum amplitude. However, in this work, this parameter is not measured directly from the absorption profile. Rather, we obtain it from Gaussian fittings. A Gaussian function is described by $F = A \exp\left(\frac{-(\lambda-\lambda_0)^2}{2\sigma^2}\right)$, with three fitting parameters. λ is the Doppler-shifted wavelength, depending on the velocity and the rest wavelength. 'A' describes the absorption depth. Dispersion σ is essentially equivalent with FWHM, except for a constant coefficient: $FWHM = 2\sqrt{2\ln 2}\sigma \approx 2.3548\sigma$. It is worth reminding again that, for convenience, we may also use the symbol ' γ ' to represent the FWHM, especially in formulas.

Uncertainty from the flux's noise (U_{flux}) is usually about 1% ~ 2%, i.e. a 50 ~ 100 Signal/Noise ratio. This uncertainty does not completely transmit to the final result, because the noise was partly smoothed off. For velocity and γ , the efficiency should be even lower, because they are not directly affected by the flux. Rather, they are determined by the wavelength which is in the perpendicular direction. For these reasons, the efficiency (r_{flux}) could be $\approx 0\%$ for V and γ . But to be strict, in this work it is set to be 30%. For A which is directly affected by the flux, we set $r_{flux} = 100\%$. The other part of uncertainty (U_{fit}) is given by fitting program in Matlab program. Total uncertainty is calculated by $U = \sqrt{(r_{flux}U_{flux})^2 + U_{fit}^2}$.

Fitting for velocity is better guided by the maximum absorption, so its uncertainty is relatively low at $< 1\%$ level, unless the pseudo-continuum was poorly determined. Fitting uncertainty of the absorption depth is usually at a level $< 2\%$. Uncertainty of FWHM is relatively higher, partly because the line blending or non-Gaussian profile. Usually it is at a level $< 5\%$. Anyway, our main targets are the trends or possible correlations, not on accurate calculation or individual object, so the errors are not really important in this study.

3 TIME EVOLUTION OF FWHM

Physically, absorption depths are mainly decided by luminosity, the ion abundance, and the energy levels. In comparison, FWHM is majorly affected by velocity vectors (note that direction also matters) in the ejecta, which decides the Doppler broadening. The velocity vectors were at least affected by temperature and collisions. These factors were likely almost determined in the explosion, barely changed afterward.

Some examples of the time evolution of FWHM are shown in Fig.1 (data and uncertainties are presented in Tab.1). The example in the upper left panel is SN 2011fe, a typical 'NV' subtype. One can see that the

evolution is very slow, especially after -8 days. Exceptions are those broad lines at early phases, for example Si II $\lambda 6355$ and Ca II NIR at $t < -6$ days. A possible reason is the saturation (Zhao et al. 2021), which can deform the absorption lines, increasing the measured FWHM. Another possible reason is the velocity, which decreases with time at early phases. FWHM may decrease accordingly, for Doppler-broadening's dependence on the velocity.

Shown in the upper right panel of Fig.1 is a typical 'HV' subtype SN Ia, the SN 2002bo. At early phases, the FWHM of Si II $\lambda 6355$ (γ^{Si6}) of this object is comparable to that of SN 2011fe (e.g. ≈ 220 Å at -12 days), but declines much slower with time. At phases near maximum light, γ^{Si6} of SN 2002bo becomes much larger than that of SN 2011fe (≈ 200 vs. 150 Å), possibly due to a higher abundance of the ion (note that the effect is less significant at early phases when the line is more saturated). Shown in the bottom left panel is the 1991T/1999aa-like object SN 1999aa. It shows a sharp decreasing of the FWHMs of Si II $\lambda 5972$ and 6355 . At -10 days, they reach a maximum of nearly 300 Å, while 6 days later, at -4 days they drop to only about 150 Å. Also note that, at -11 days, the FWHM of Ca II NIR is relatively small. A direct reason is very weak absorption ($pEW \lesssim 10\%$), possibly due to too high temperature. Finally, an example of 1991bg-like object, the SN 1999by, is shown in the bottom right panel. As one can see, the FWHM of Si II $\lambda 6355$ increases with time at phases near maximum light. Though the reason is unclear, we do see similar trend of the velocity in our previous work Zhao et al. (2021).

4 CORRELATION WITH REST WAVELENGTH

Fig.2 shows how FWHM correlates with the rest-wavelength. Rest-wavelength is $3945, 4130, 5454\&5620, 5972, 6355, 8567$ Å for Ca II HK, Si II $\lambda 4130$, S II W-trough, Si II $\lambda 5972$, Si II $\lambda 6355$ and Ca II NIR, respectively. It is clear that shorter lines have a narrower FWHM. Therefore, a speculation is that wavelength may play an important role. In fact, the widths of absorption features are mainly decided by Doppler-broadening, which originated from kinetic motions, including thermal motion and turbulence. A rough expression is $\Delta\lambda \approx \frac{\Delta V}{c}\lambda_0$, where ' V ' is the velocity, ' c ' is the speed of light. Obviously, it is proportional to the rest-wavelength λ_0 .

Since the rest wavelength is decided by the excitation energy, i.e. $E_{exc} = \frac{hc}{\lambda}$, in essence FWHM is dependent on the excitation energy. And, since $pEW \approx 1.064\gamma$ (for Gaussian profiles), the line strengths should also depend on the excitation energy. This, actually, has been confirmed by previous measurement results (see for example, Zhao et al. 2021, 2024).

In Fig.2, the ratio of FWHM to wavelength, $R = \gamma/\lambda_0$, is shown as a function of the time. Generally speaking, the ratio is close to 0.015 for all lines, and barely evolve with time after -6 days. Median errors (which is less affected by outliers) are $\approx 0.0007, 0.0006, 0.0017, 0.0016, 0.0017, 0.0018, 0.0005$, for lines S II $\lambda 5454$, S II $\lambda 5620$, Si II $\lambda 4130$, Si II $\lambda 5972$, Si II $\lambda 6355$, Ca II HK, and Ca II NIR, respectively. In other words, the error level is mostly below 10%.

In the below panel of Fig.2, we show a scaled version of the ratio R . The scaling factor is expressed as an exponential function $e^{-0.29(E_{exc} - E_{exc}^{Si6})}$. This further reduces their differences, especially after -5 days, except for line Ca II HK. The reason is unclear, though this line does have some specificity, like almost zero lower level, and very short wavelength $\lambda \approx 3945$ Å.

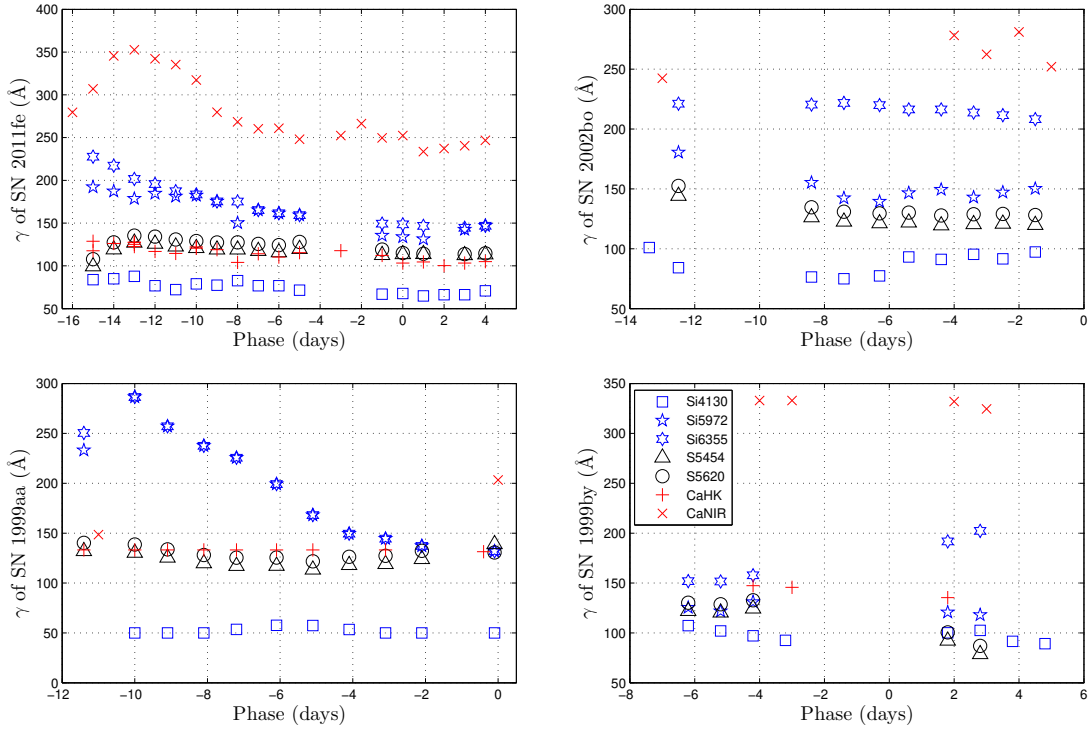


Fig. 1: Time evolutions of the FWHMs (γ) of SN 2011fe (upper left panel, NV subtype), SN 2002bo (upper right panel, HV subtype), SN 1999aa (lower left panel, 1991T/1999aa subtype) and SN 1999by (lower right panel, NV subtype). Marker specifiers: the square, pentagram, hexagram, triangle, plus and cross mark the absorption features Si II λ 4130, Si II λ 5972, Si II λ 6355, S II λ 5454, S II λ 5620, Ca II HK and Ca II NIR, respectively.

The relation between FWHM and the wavelength can be helpful in spectral measurements. Usually, the velocities of the lines are easier to be determined, while FWHM, or σ in the Gaussian function is harder to determine, especially when line blending is serious. An example is the fitting of Si II λ 5972. This line is relatively weak, and to some extent affected by HVF of Si II λ 6355 (or some unknown absorption that lies between Si II λ 5972 and Si II λ 6355). This often makes it difficult to accurately determine the FWHM of Si II λ 5972. In comparison, FWHM of Si II λ 6355 is often much easier to determine, if its HVF is not too strong. Therefore, we may use the FWHM of Si II λ 6355 to help determine that of Si II λ 5972.

5 DIVERSITY AMONG DIFFERENT SUBCLASSES

As mentioned before, diversity of SN Ia can be roughly indicated by the velocity. Usually, those with relatively higher velocities also have larger line strengths (Wang et al. 2009). Physically, the line strength represents absorption rate of the photons, which is mainly determined by the abundance of the absorbing ions and the energy levels of their electrons. Therefore, HV SNe may have more abundant IMEs in their ejecta. Now, a key question is whether higher velocity also results in a larger FWHM. The results of our investigation is shown in the left panel of Figure 3 (data are presented in Tab.2). Apparently, indeed HV objects have relatively larger FWHM. This result is expected, as Doppler broadening depends on the ejecta's velocity.

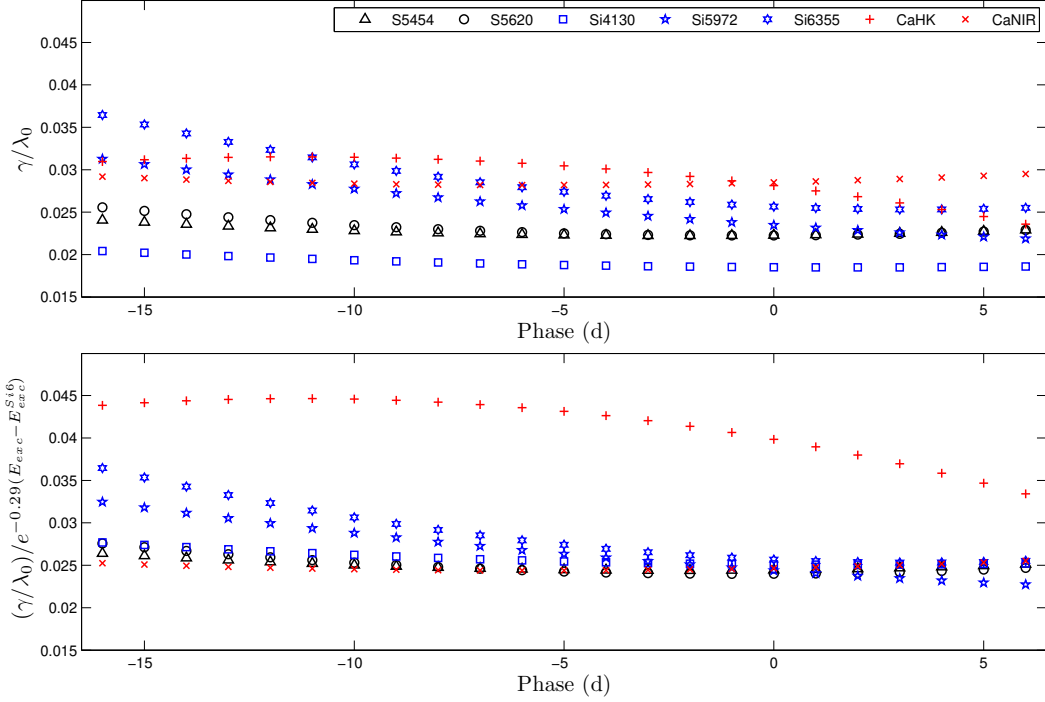


Fig. 2: Shown in the upper panel are fitting results of the ratios of FWHMs and wavelengths ($R = \gamma/\lambda_0$) for several lines. Data are mostly from the sample presented in Zhao et al. (2021, 2024) and fitted with second-order polynomials. But, the sample size is too large, and we are only interested in the overall trend, so they are not fully presented in Tab.1 & 2. Shown below is also the ratio, but scaled by a factor of $e^{-0.29(E_{exc} - E_{exc}^{Si6})}$, where ‘ E_{exc} ’ is the line’s excitation energy (i.e. $\frac{hc}{\lambda_0}$), and ‘ E_{exc}^{Si6} ’ is that of line Si II $\lambda 6355$.

In the right panel, we show a few typical objects. One can see that for each object, FWHM basically increases with the velocity. This is expected, as Doppler broadening (which is determined by velocity distributions in the ejecta) is the main origin of the FWHM. However, if the velocity is the same, then it appears that NV object tends to have larger FWHM than HV objects. A possible reason is that NV objects would then typically appear at earlier phases, when the temperatures could be relatively higher. An additional evidence is that 1991T/1999aa-like objects show the largest FWHM. At first glance, these might seem opposite to those in the left panel, but in fact, they only reflect the fact that other factors (other than the absolute value of velocity) also affect the FWHM. It should also be noted that here the comparison is not necessarily at the same phase. For NV objects in the right panel, the correlation is fitted as $\gamma \approx 0.02V - 50$, where ‘ V ’ is the velocity (km/s). Cold 1991bg-like objects show low velocity and also low FWHM.

A four-days change of FWHM is shown in the upper panel of Fig.4, as a function of the decline rate (data are from Tab.2). Apparently, 1991T/1999aa-like objects show much greater variation than other objects. This is understandable, as higher explosion temperature is expected to cause greater Doppler broadening than colder objects. This regulation can help identify the subtype. An example is SN 2006S which is easily mistaken for a NV object. As shown in the upper panels of Fig.4, this object actually has a very rapid variation of FWHM, which is a sign of 1991T/1999aa-like object. A more direct evidence is, of course, its relatively high luminosity ($\Delta m_{15} \approx 0.9$ mag). A similar case is the outlier SN 2012fr in the left panel

of Fig.3, which also shows a rapid decrease of the FWHM of Si II $\lambda 6355$ (an approximating polynomial of degree 2 suggests $\gamma^{Si6} \approx 193 \text{ \AA}$ at -4 days, and $\approx 168 \text{ \AA}$ at 0 days, so $\Delta\gamma^{Si6}/\Delta t \approx 6.3 \text{ \AA/d}$) and a very bright luminosity ($\Delta m_{15} \approx 0.8 \text{ mag}$). So, we also consider it a 1991T/1999aa-like object, rather than ‘HV’. More detailed observations and profound analysis of this object can be found in e.g. Childress et al. (2013); Zhang et al. (2014). In the lower panel of Fig.4, the FWHM of Si II $\lambda 5972$ at maximum light is plotted against the decline rate. No clear correlation is seen, meaning the FWHM is possibly independent of the decline rate, or only insignificantly affected.

6 POSSIBLE APPLICATIONS OF THE FWHM

In most studies, the absorption strength was represented with pEW. But in fact, its correlation with Δm_{15} is weaker than the maximum absorption depth. A possible reason is that, pEW is also affected by FWHM which has a relatively high uncertainty (see Section 2). As mentioned before, the most sensitive indicator of the decline rate may be A^{Si5} . An example is shown in the upper left panel of Figure 5 (phases are at $|t| \leq 1$ days; data are presented in Tab.3). Based on the residuals from the fit, the sample is split into two groups: the inliers with $\Delta A^{Si5} = |A^{Si5} - A_{fitted}^{Si5}| \leq 0.07$ and the outliers with $\Delta A^{Si5} > 0.07$. As shown in the upper right panel, the outliers are predominantly found at $\gamma^{Si5} > 130 \text{ \AA}$. This means that objects with $\gamma^{Si5} \leq 130 \text{ \AA}$ are predominantly inliers in the $A^{Si5}-\Delta m_{15}$ correlation. Also, they appear to span a narrower range of A^{Si5} , typically from 0.05 to 0.25. In comparison, objects with $\gamma^{Si5} > 130 \text{ \AA}$ span a broader range of A^{Si5} , typically from 0.05 to 0.40. These results may imply relatively low diversity among these objects with $\gamma^{Si5} \leq 130 \text{ \AA}$. The reason is unclear, but a more symmetry explosion, with less collisions, may lead to less velocity dispersion and so a smaller FWHM. Also, interfering factors like saturation may be weaker in these objects. Anyway, if they are truly a more homogeneous sample, then one may consider using such a smaller sample to calibrate the cosmic distance.

Many spectral parameters have been found to have a strong correlation with the decline rate, which can be used to estimate the brightness. But this, in fact, is not practicable, because usually the spectral parameters significantly vary with time. And, determining the phase itself requires light curve, the lack of which is the very reason that we have to use a spectroscopic method. For example, the ‘Si II ratio’ $R_{si} = A^{Si5}/A^{Si6}$ as defined by (Nugent et al. 1995) also has a strong correlation with Δm_{15} (Pearson’s correlation coefficient $\rho = 0.918$ for ‘good’ candidates in Fig.5), but its time evolution is very significant (mostly due to the evolution of Si II $\lambda 6355$). A_{Si5} has the strongest correlation with Δm_{15} ($\rho = 0.951$), and also one of the slowest evolution, but the error level is still too high. The best choice may be the ratio of depth to FWHM of Si II $\lambda 5972$ ($R_{A\gamma}^{Si5} = A^{Si5}/\gamma^{Si5}$). This ratio has a strong correlation with Δm_{15} ($\rho = 0.910$), and luckily, also a very slow temporal evolution, as shown in the lower left panel of Fig.5. The ratio can be considered as a shape index (the larger it is, the sharper the curve is), so its quasi-invariance suggests that the absorption features vary in a self-similar style. Average value of $R_{A\gamma}^{Si5}$ is near 0.002 \AA . The increase near maximum light may be partially due to increase of dimmer objects in the sample. Assuming that the spectrum is obtained at phases between -15 days to +5 days, a rough estimation is $\Delta m_{15} \approx 0.725 + 373A^{Si5}/\gamma^{Si5}$. The formula is fitted from those ‘good candidates’ in the lower-right panel of Fig.5. A test with 883 spectra yields median absolute errors (i.e. 50%-confidence uncertainty, here

we did not use standard deviation, for too large influence from outliers) $\tilde{E} \lesssim 0.20$ mag at $t \leq -10$ days, and $\tilde{E} \lesssim 0.11$ mag at $-10 \leq t \leq +3$ days. A further improvement is still possible, if line Si II $\lambda 5972$ is further studied, or taking into consideration other factors like the subtype, but this is beyond the scope of this study.

7 CONCLUSION

Spectral features of SNe Ia carry important information about the explosion. But unfortunately, they are difficult to interpret, as multiple factors affect. In this study, we focus on an important one, i.e. the FWHM of the absorption features. It is a crucial parameter for spectral fitting. And, together with absorption depth, it decides the line strength.

Our results suggest that, FWHM is mainly determined by the wavelength of the line, or equivalently the excitation energy. Difference in FWHM can be significantly reduced by dividing their wavelengths. The reason may be Doppler broadening, which is roughly expressed as $\Delta\lambda \approx \frac{\Delta v}{c}\lambda_0$. We also found that, further scaling with a factor $e^{-0.29(E_{exc} - E_{exc}^{Si6})}$ can further reduce the difference of FWHM among lines Si II $\lambda\lambda$ 4130, 5972, 6355, Ca II NIR, and the two lines of S II W-trough. The only exception is Ca II HK which itself is special for having almost zero E_{lower} and the shortest wavelength. This correlation is helpful in fitting lines that are seriously blended, for example the important line Si II $\lambda 5972$.

Besides wavelength, FWHM is also affected by velocity and possibly the temperature. Generally speaking, higher velocity often corresponds to larger FWHM. And, higher temperature may be the reason that 1991T/1999aa-like objects show the largest FWHM, if compared at the same velocity. 1991T/1999aa-like objects also show much faster time evolution of FWHM, which may be used to help identify the subtype.

We found that, objects with FWHM of Si II $\lambda 5972$ smaller than 130 \AA have much tighter correlation between the absorption depth of Si II $\lambda 5972$ and Δm_{15} . This may suggest a new constrain on the sample to further improve the accuracy of distance's measurement in cosmology.

We also found that Si II $\lambda 5972$ happens to have a relatively slow time evolution. So, in case when light curve is not available, a very rough estimation can be obtained from relation $\Delta m_{15} \approx 0.725 + 373A^{Si5}/\gamma^{Si5}$ (assuming that the phase is between -15 and +5 days).

ACKNOWLEDGEMENTS

We thank the anonymous referee, for comments which significantly elevated the level of this paper. This research has made use of the CfA Supernova Archive, which is funded in part by the National Science Foundation through grant AST 0907903, the Berkeley/Lick Supernova Archives, which is funded in part by the US National Science Foundation, and the CSP Supernova Archive, which is supported by the World Premier International Research Center Initiative. Here we express our deep gratitude.

References

- Benetti S. et al., 2005, ApJ, 623, 1011 2
- Blondin S. et al., 2012, AJ, 143, 126 3
- Blondin S., Dessart L., Hillier D. J., 2018, MNRAS, 474, 3931 2

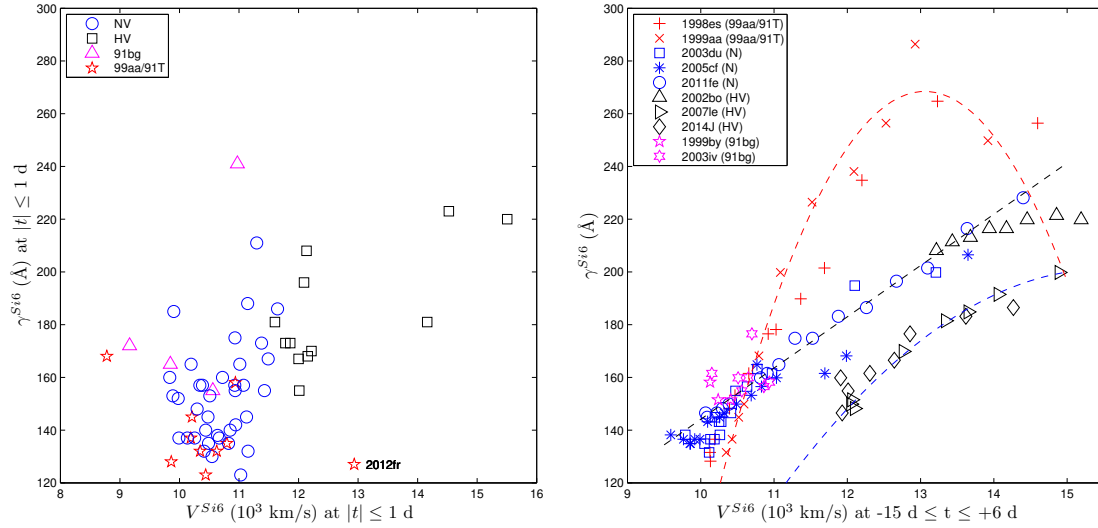


Fig. 3: . Correlation between the velocity and FWHM of Si II λ 6355. Left panel: A sample at phases near maximum light, i.e. $|t| \leq 1$ days. Each point represents an individual object. Right panel: Some typical objects, at phases $\leq +6$ days. Classifications are according to Wang et al. (2009).

Branch, D., et al. 2006, PASP, 118, 560 2

Branch D., Dang L. C., Baron E., 2009, PASP, 121, 238 2

Childress, M. J., Scalzo, R. A., Sim, S., et al. 2013, ApJ, 770, 29 7

Childress M. J., Filippenko A. V., Ganeshalingam M., Schmidt B. P., 2014, MNRAS, 437, 338 2

Filippenko A. V. et al., 1992, Astron. J., 104, 1543 2

Filippenko A. V. et al., 1992, Astrophys. J., 384, L15 2

Flörs A. et al., 2020, MNRAS, 491, 2902 1, 2

Folatelli G. et al., 2013, ApJ, 773, 53 3

Freedman W. L. et al., 2019, ApJ, 882, 34 1

Hakobyan A. A., Gevorgyan M. H., Karapetyan A. G. et. al., 2025, arXiv:2511.23305 2

Hillebrandt W., Niemeyer J. C., 2000, ARA&A, 38, 191 1

Iben I., Tutukov A. V., 1984, ApJS, 54, 355 2

Jha S. W., Maguire K., Sullivan M., 2019, Nature Astron., 3, 706 1

Ruiz-Lapuente P., González Hernández, J. I., Cartieret R. et. al., 2023, ApJ947 90 2

Khokhlov, A. M., 1991, A&A, 245, 114 1

Kushnir D., Katz B., Dong S., Livne E., Fernández R., 2013, ApJ, 778, L37 1

Li W., Filippenko A. V., Treffers R. R., Riess A. G., Hu J., & Qiu Y., 2001, ApJ, 546, 734 2

Li W. et al., 2011, Nature, 480, 348 2

Maeda K. et al., 2010, Nature, 466, 82 1

Maeda K., Jiang J., Shigeyama T., Doi M., 2018, ApJ, 861, 78 1

Maguire K. et al., 2014, MNRAS, 444, 3258 2

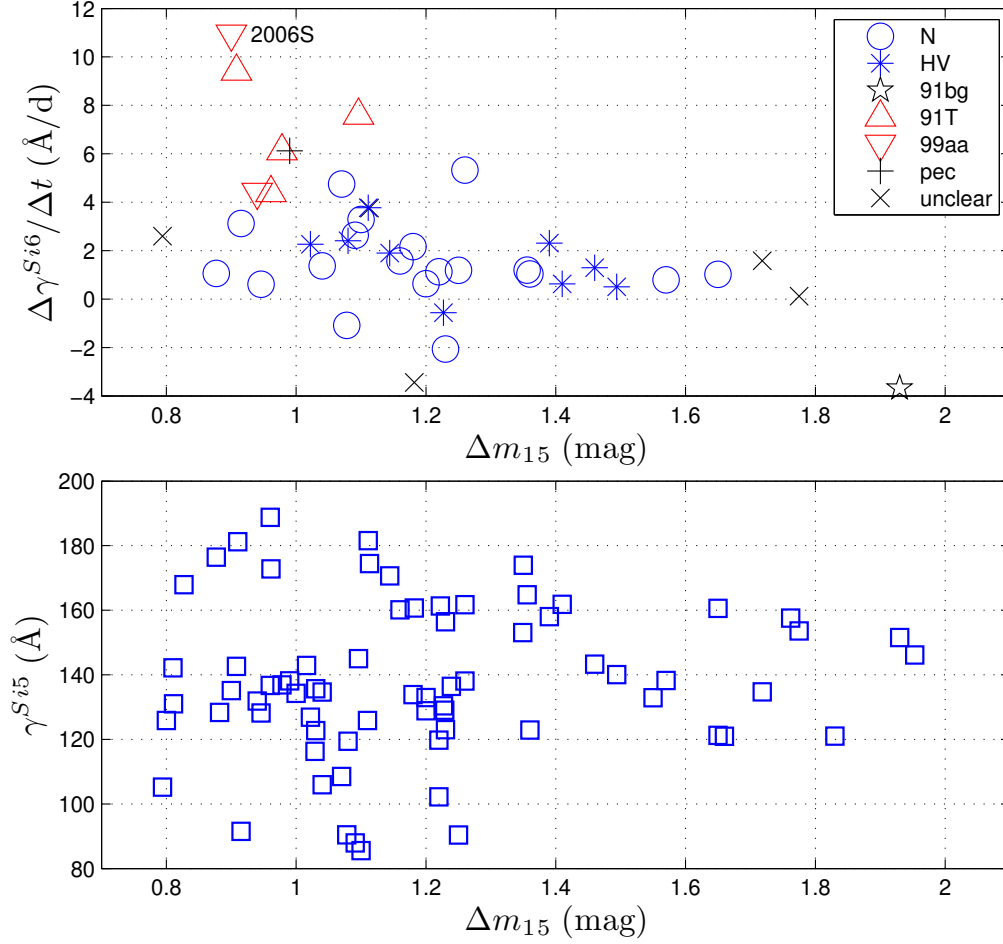


Fig. 4: Upper panel: decline rate of FWHM of Si II $\lambda 6355$ ($\Delta\gamma^{Si6}/\Delta t$) as a function of the decline rate of brightness (Δm_{15}). Here $\Delta\gamma^{Si6}$ is calculated by $\Delta\gamma^{Si6} = \gamma_{t_1}^{Si6} - \gamma_{t_2}^{Si6}$, with $t_1 \approx -4$ days and $t_2 \approx 0$ days. Δt is calculated by $\Delta t = t_2 - t_1$. Lower panel: Δm_{15} vs. the FWHM of Si II $\lambda 5972$ of SNe Ia at the time of B-band maximum light.

Matheson T. et al., 2008, AJ, 135, 1598 3

Ni Y. et al, 2023, ApJ, 959, 132 2

Nomoto K., 1982, ApJ, 253, 798 1, 2

Nugent P., Phillips M., Baron E., Branch D., Hauschildt P. 1995, ApJ, 455, L147 7

Pakmor R., Kromer M., Taubenberger S., Springel V., 2013, ApJ, 770, L8 1

Perlmutter S. et al., 1999, ApJ, 517, 565 1

Phillips M. M. et al., 1992, Astron. J., 103, 1632 2

Phillips M. M., 1993, ApJ, 413, L105 1

Phillips M. M. et al., 1999, AJ, 118, 1766 1

Riess A. G. et al., 1998, AJ, 116, 1009 1

Riess A. G., Casertano S., Yuan W., Macri L. M. Scolnic D., 2019, ApJ, 876, 85 1

Shen K. J., Kasen D., Miles B. J., Townsley D. M., 2018, ApJ, 854, 52 2

Silverman J. M. et al., 2012a, MNRAS, 425, 1789 3

Silverman J. M., Kong J. J., Filippenko A. V., 2012b, MNRAS, 425, 1819 3

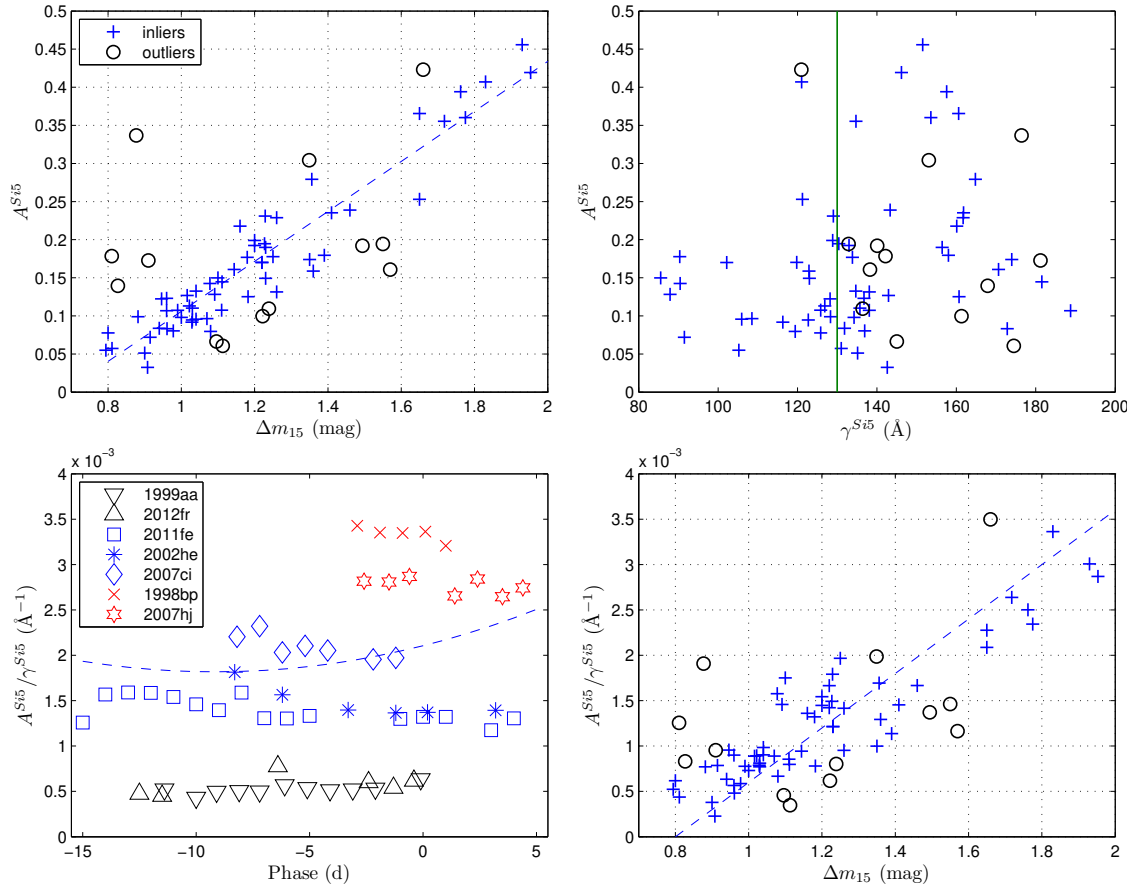


Fig. 5: Upper left panel shows the absorption depth of Si II $\lambda 5972$ (A^{Si5}) as a function of the decline rate (Δm_{15}). Plus signs mark the inliers which have relatively small residuals from the fit, i.e. $\Delta A^{Si5} = |A^{Si5} - A^{Si5}_{fitted}| \leq 0.07$, where A^{Si5}_{fitted} is given by the best-fit linear relation. Black circles mark the outliers which have relatively large residuals, i.e. $\Delta A^{Si5} = |A^{Si5} - A^{Si5}_{fitted}| > 0.07$. All objects are measured at $|t| \leq 1$ days, each point represents an individual object. The straight dash line in this panel is only a guiding line, not a fitting line. Upper right panel shows A^{Si5} as a function of the FWHM (γ^{Si5}). Markers in this panel and the lower right panel are the same as for the upper left panel. Lower left panel shows the temporal evolution of the ratio of depth to FWHM of line Si II $\lambda 5972$ (A^{Si5}/γ^{Si5}). The dash line in this panel is a fitting line with a large sample (data not completely presented in this paper, for the same reason as in Fig.2). Lower right panel shows the correlation between A^{Si5}/γ^{Si5} and the decline rate. The straight dash line in this panel is also a guiding lines.

Silverman J. M. et al., 2015, MNRAS, 451, 1973 2

Wang X. et al., 2009, ApJ, 699, L139 2, 5, 9

Webbink R. F., 1984, ApJ, 277, 355 2

Whelan J., Iben I., 1973, ApJ, 186, 1007 2

Meng X., 2019, ApJ, 886, 58 2

Zhang J., Wang X., Bai J. et al., 2014, AJ, 148, 1 7

Zhao X. et al., 2015, ApJS, 220, 20 2

Zhao X. et al., 2016, ApJ, 826, 211 3

Zhao X. et al., 2021, MNRAS, 503, 4667 2, 4, 6, 14

Zhao X. et al., 2024, MNRAS, 535, 3470 3, 4, 6, 14

Table 1: Temporal evolution of the FWHMs of several important absorption features of SN 2011fe

SN	Phase (days)	γ^{Si4} (Å)	γ^{Si5} (Å)	γ^{Si6} (Å)	γ^{S1} (Å)	γ^{S2} (Å)	γ^{CaHK} (Å)	γ^{CaNIR} (Å)
1999aa	–	–	233(11)	251(4)	132(7)	140(4)	133(7)	–
1999aa	–	–	–	–	–	–	–	149(11)
1999aa	-10	50(3)	286(15)	286(3)	130(7)	139(4)	133(7)	–
1999aa	-9.1	50(3)	257(13)	257(2)	125(7)	134(2)	133(7)	–
1999aa	-8.1	50(3)	238(12)	238(2)	120(15)	128(12)	133(7)	–
1999aa	-7.2	54(3)	226(12)	226(3)	117(6)	125(2)	133(7)	–
1999aa	-6.1	58(3)	199(11)	199(2)	117(6)	126(2)	133(7)	–
1999aa	-5.1	57(2)	168(9)	168(9)	113(6)	122(7)	133(7)	–
1999aa	-4.1	53(2)	150(8)	150(8)	118(6)	126(7)	–	–
1999aa	-3.1	50(3)	145(8)	145(8)	119(6)	127(7)	133(7)	–
1999aa	-2.1	50(3)	137(7)	137(7)	124(7)	132(7)	–	–
1999aa	–	–	–	–	–	–	131(4)	–
1999aa	-0.1	50(3)	132(7)	132(7)	139(7)	131(7)	–	–
1999aa	–	–	–	–	–	–	–	203(6)
1999by	-6.2	107(6)	125(6)	152(2)	122(7)	130(4)	–	–
1999by	-5.2	102(6)	122(4)	152(2)	120(7)	129(2)	–	–
1999by	-4.2	97(6)	131(4)	158(2)	124(7)	133(2)	147(8)	–
1999by	–	–	–	–	–	–	–	333(18)
1999by	-3.2	93(6)	–	–	–	–	–	–
1999by	–	–	–	–	–	–	146(8)	333(18)
1999by	1.8	100(9)	121(7)	192(10)	92(5)	101(6)	135(8)	–
1999by	–	–	–	–	–	–	–	332(12)
1999by	2.8	103(9)	118(6)	202(11)	79(4)	87(5)	–	–
1999by	–	–	–	–	–	–	–	325(11)
1999by	3.8	92(9)	–	–	–	–	–	–
1999by	4.8	89(9)	–	–	–	–	–	–
2002bo	-13.4	101(4)	–	–	–	–	–	–
2002bo	–	–	–	–	–	–	–	242(6)
2002bo	-12.5	84(4)	181(10)	221(12)	144(8)	152(8)	–	–
2002bo	-8.4	76(2)	155(8)	220(12)	126(7)	135(7)	–	–
2002bo	-7.4	75(6)	142(8)	222(12)	123(7)	131(7)	–	–
2002bo	-6.3	77(2)	139(7)	220(12)	121(7)	130(7)	–	–
2002bo	-5.4	93(2)	147(8)	216(11)	122(7)	130(7)	–	–
2002bo	-4.4	91(2)	149(8)	216(11)	119(6)	128(7)	–	–
2002bo	–	–	–	–	–	–	–	278(4)
2002bo	-3.4	95(2)	143(8)	214(11)	121(7)	129(7)	–	–

2002bo	–	–	–	–	–	–	–	262(4)
2002bo	-2.5	92(2)	147(8)	212(11)	121(7)	129(7)	–	–
2002bo	–	–	–	–	–	–	–	281(6)
2002bo	-1.5	97(2)	150(8)	208(11)	120(7)	128(7)	–	–
2002bo	–	–	–	–	–	–	–	252(6)
2011fe	–	–	–	–	–	–	–	280(3)
2011fe	-15	84(5)	192(7)	228(2)	99(6)	108(4)	129(7)	307(2)
2011fe	-14	85(4)	187(6)	217(2)	119(6)	127(4)	126(7)	346(2)
2011fe	-13	88(4)	179(4)	202(2)	127(7)	135(2)	128(7)	353(4)
2011fe	-12	77(4)	185(4)	196(2)	126(7)	134(2)	117(6)	342(6)
2011fe	-11	72(4)	181(4)	187(2)	123(7)	131(2)	115(6)	335(4)
2011fe	-10	79(4)	182(4)	183(2)	121(7)	129(2)	121(7)	317(4)
2011fe	-9	77(4)	175(6)	175(2)	119(6)	127(2)	119(6)	280(4)
2011fe	-8	83(5)	150(8)	175(2)	119(6)	127(2)	104(2)	268(4)
2011fe	-7	77(4)	165(9)	165(2)	117(6)	126(2)	114(4)	260(4)
2011fe	-6	77(4)	161(9)	161(2)	116(4)	124(4)	110(4)	261(4)
2011fe	-5	72(2)	159(8)	159(2)	120(6)	128(4)	115(4)	248(4)
2011fe	–	–	–	–	–	–	118(2)	252(4)
2011fe	–	–	–	–	–	–	–	266(14)
2011fe	-1	67(2)	135(6)	149(2)	113(4)	119(2)	112(2)	250(2)
2011fe	0	68(2)	134(7)	149(3)	114(4)	115(2)	103(2)	252(2)
2011fe	1	65(2)	131(7)	147(8)	114(6)	114(6)	105(2)	234(4)
2011fe	2	66(2)	–	–	–	–	100(2)	237(4)
2011fe	3	66(2)	143(8)	145(8)	112(6)	114(6)	103(6)	240(4)
2011fe	4	71(2)	147(8)	147(8)	113(6)	115(6)	105(6)	247(4)

Note: Data sources and photometric parameters can be found in Zhao et al. (2021, 2024). Phases are from the B -band maximum light. γ represents the full with half maximum (FWHM). Superscripts ‘ $Si4$ ’, ‘ $Si5$ ’, ‘ $Si6$ ’, ‘ $S1$ ’, ‘ $S2$ ’, ‘ $CaHK$ ’ and ‘ $CaNIR$ ’ mark lines Si II $\lambda 4130$, Si II $\lambda 5972$, Si II $\lambda 6355$, S II $\lambda 5454$, S II $\lambda 5620$, Ca II HK and Ca II NIR, respectively.

Table 2: The velocities and FWHMs of Si II $\lambda 6355$

SN	Phase	V^{Si6}	γ^{Si6}	subtype	Δm_{15}	SN	Phase	V^{Si6}	γ^{Si6}	subtype	Δm_{15}
	(days)	(km/s)	(\AA)		(mag)		(days)	(km/s)	(\AA)		(mag)
1986G	-4	11555(127)	188(10)	NV	1.65	2003du	-0.1	10133(119)	136(7)	NV	1.07
1986G	0	9904(109)	184(10)	NV	1.65	2003it	-3.3	11734(86)	158(3)	NV	1.36
1992A	-4	12579(122)	176(3)	HV	1.41	2003it	-0.2	11428(67)	155(2)	NV	1.36
1992A	0	11860(170)	173(9)	HV	1.41	2003iv	-2.5	10938(215)	158(4)	91bg	1.65

Continued on next page

Table 2 continued

SN	Phase (days)	V^{Si6} (km/s)	γ^{Si6} (Å)	subtype	Δm_{15} (mag)	SN	Phase (days)	V^{Si6} (km/s)	γ^{Si6} (Å)	subtype	Δm_{15} (mag)
1995E	-4.2	11118(142)	166(9)	NV	1.16	2003iv	-1.9	10862(163)	157(9)	91bg	1.65
1995E	-0.2	10722(135)	160(9)	NV	1.16	2003iv	-1.5	10862(163)	157(9)	91bg	1.65
1996X	-4.1	11188(65)	160(2)	NV	1.26	2003iv	-0.9	10649(153)	160(9)	91bg	1.65
1996X	-0.1	10640(107)	138(3)	NV	1.26	2003iv	-0.5	10649(153)	160(9)	91bg	1.65
1997bp	-3.1	16000(174)	226(12)	HV	1.08	2003iv	0.1	10561(163)	155(3)	91bg	1.65
1997bp	-0.2	15506(167)	219(11)	HV	1.08	2003iv	0.5	10561(163)	155(3)	91bg	1.65
1997dt	-4.8	11649(43)	163(2)	NV	1.04	2003iv	1.1	10510(131)	160(3)	91bg	1.65
1997dt	0.2	10929(118)	156(8)	NV	1.04	2003iv	1.5	10510(131)	160(3)	91bg	1.65
1998de	-3.2	11865(208)	230(5)	91bg	1.93	2003iv	1.6	10699(130)	177(9)	91bg	1.65
1998de	-0.3	10973(160)	241(13)	91bg	1.93	2003iv	3.5	10152(139)	162(3)	91bg	1.65
1998dh	-3.5	12000(131)	165(9)	HV	1.227	2004as	-4	12797(170)	212(11)	HV	1.111
1998dh	-0.5	12000(131)	166(9)	HV	1.227	2004as	-0.1	12092(152)	197(10)	HV	1.111
1998es	-11.5	14598(90)	256(3)	91T	0.978	2004at	-3.7	10978(127)	155(8)	NV	1.091
1998es	-10.4	13231(84)	265(3)	91T	0.978	2004at	0.2	10480(53)	145(2)	NV	1.091
1998es	-9.4	12200(129)	235(2)	91T	0.978	2004gs	-3.8	11678(178)	196(11)	unclear	1.775
1998es	-8.5	11689(60)	201(4)	91T	0.978	2004gs	-0.3	10893(168)	195(11)	unclear	1.775
1998es	-7.4	11365(118)	190(10)	91T	0.978	2005cf	-12.7	13648(65)	206(2)	NV	1.1
1998es	-6.4	11028(117)	178(9)	91T	0.978	2005cf	-10.7	11989(129)	168(9)	NV	1.1
1998es	-5.4	10921(115)	177(9)	91T	0.978	2005cf	-9.7	11695(127)	162(9)	NV	1.1
1998es	-4.5	10656(112)	162(9)	91T	0.978	2005cf	-7.7	11033(126)	160(9)	NV	1.1
1998es	-3.4	10468(39)	153(2)	91T	0.978	2005cf	-6.7	10767(94)	165(3)	NV	1.1
1998es	-2.4	10392(112)	148(8)	91T	0.978	2005cf	-5.7	10829(58)	157(2)	NV	1.1
1998es	-0.5	10190(109)	137(7)	91T	0.978	2005cf	-4.7	10689(59)	153(2)	NV	1.1
1998es	0.5	10126(107)	132(7)	91T	0.978	2005cf	-3.7	10488(61)	150(2)	NV	1.1
1998es	1.5	10133(110)	128(7)	91T	0.978	2005cf	-2.7	10320(56)	147(2)	NV	1.1
1998es	-4.5	10656(112)	161(9)	91T	0.978	2005cf	-1.7	10257(52)	145(2)	NV	1.1
1998es	-0.5	10190(109)	137(7)	91T	0.978	2005cf	-0.7	10094(60)	143(2)	NV	1.1
1999aa	-11.4	13919(116)	250(4)	99aa	0.94	2005cf	0.3	9990(54)	137(2)	NV	1.1
1999aa	-10	12927(72)	286(3)	99aa	0.94	2005cf	1.3	9918(53)	137(2)	NV	1.1
1999aa	-9.1	12528(57)	256(2)	99aa	0.94	2005cf	2.3	9852(112)	135(7)	NV	1.1
1999aa	-8.1	12092(57)	238(2)	99aa	0.94	2005cf	3.3	9860(111)	135(7)	NV	1.1
1999aa	-7.2	11520(68)	226(3)	99aa	0.94	2005cf	4.3	9765(117)	137(7)	NV	1.1
1999aa	-6.1	11087(65)	200(2)	99aa	0.94	2005cf	5.3	9592(119)	138(7)	NV	1.1
1999aa	-5.1	10795(116)	168(9)	99aa	0.94	2005cf	-3.7	10488(61)	150(2)	NV	1.1
1999aa	-4.1	10592(112)	150(8)	99aa	0.94	2005cf	0.3	9990(54)	137(2)	NV	1.1
1999aa	-3.1	10518(111)	145(8)	99aa	0.94	2006N	-3.4	11474(125)	158(8)	NV	1.57

Continued on next page

Table 2 continued

SN	Phase (days)	V^{Si6} (km/s)	γ^{Si6} (Å)	subtype	Δm_{15} (mag)	SN	Phase (days)	V^{Si6} (km/s)	γ^{Si6} (Å)	subtype	Δm_{15} (mag)
1999aa	-2.1	10428(111)	137(7)	99aa	0.94	2006N	0.7	10935(123)	155(8)	NV	1.57
1999aa	-0.1	10348(112)	132(7)	99aa	0.94	2006S	-4.7	11805(144)	190(10)	99aa	0.9
1999aa	-4.1	10592(112)	150(8)	99aa	0.94	2006S	0.3	10797(128)	135(7)	99aa	0.9
1999aa	-0.1	10348(112)	132(7)	99aa	0.94	2006bt	-4	12224(141)	216(11)	NV	0.877
1999ac	-4	11070(36)	163(2)	unclear	1.182	2006bt	-0.1	11298(157)	212(11)	NV	0.877
1999ac	-1	10168(40)	173(2)	unclear	1.182	2006sr	-3	12477(137)	175(9)	HV	1.39
1999by	-6.2	10408(48)	152(2)	91bg	1.899	2006sr	-1	12218(143)	170(9)	HV	1.39
1999by	-5.2	10239(58)	152(2)	91bg	1.899	2007A	-3.5	10791(76)	142(2)	NV	0.946
1999by	-4.2	10128(61)	158(2)	91bg	1.899	2007A	0.4	10441(71)	140(2)	NV	0.946
1999by	1.8	8978(103)	191(10)	91bg	1.899	2007S	-3.8	10625(118)	168(9)	91T	1.096
1999by	2.8	8876(98)	201(11)	91bg	1.899	2007S	-0.8	10211(115)	145(8)	91T	1.096
1999cc	-3.2	12177(182)	186(10)	HV	1.46	2007af	-3.7	10854(122)	159(9)	NV	1.2
1999cc	-0.2	11604(169)	182(10)	HV	1.46	2007af	0.3	10386(125)	157(8)	NV	1.2
1999cl	-4.3	13081(138)	217(11)	HV	1.144	2007le	-10.4	14892(168)	200(11)	HV	1.015
1999cl	0.7	12135(128)	207(11)	HV	1.144	2007le	-8.4	14060(156)	191(10)	HV	1.015
1999dq	-3.5	10485(111)	140(8)	91T	0.961	2007le	-7.5	13649(147)	185(10)	HV	1.015
1999dq	0.5	10441(110)	123(7)	91T	0.961	2007le	-6.5	13341(144)	181(10)	HV	1.015
1999gp	-4.9	11918(149)	204(11)	91T	0.908	2007le	-4.7	12764(135)	170(9)	HV	1.015
1999gp	0	10939(82)	158(3)	91T	0.908	2007le	2.3	12061(149)	152(8)	HV	1.015
2000cx	-3.8	13856(79)	163(4)	pec	0.99	2007le	3.3	12098(138)	148(8)	HV	1.015
2000cx	0.2	13692(53)	138(2)	pec	0.99	2007le	4.3	12048(141)	150(8)	HV	1.015
2000dk	-4.3	11606(131)	179(10)	unclear	1.718	2008Q	-3.3	11473(61)	148(2)	NV	1.25
2000dk	0.4	10675(118)	172(9)	unclear	1.718	2008Q	-0.3	11126(63)	145(2)	NV	1.25
2001cp	-4	11218(137)	146(8)	NV	0.915	2008ar	-3.7	10497(157)	149(8)	NV	1.078
2001cp	0.9	10547(130)	130(7)	NV	0.915	2008ar	-0.7	10510(140)	153(8)	NV	1.078
2001ep	-3.2	10671(118)	168(9)	NV	1.356	2011fe	-15	14401(48)	228(2)	NV	1.18
2001ep	-0.2	10195(115)	165(9)	NV	1.356	2011fe	-14	13636(44)	216(2)	NV	1.18
2002bo	-12.5	17000(196)	221(12)	HV	1.08	2011fe	-13	13097(45)	201(2)	NV	1.18
2002bo	-8.4	15192(173)	220(12)	HV	1.08	2011fe	-12	12671(25)	196(2)	NV	1.18
2002bo	-7.4	14857(160)	221(12)	HV	1.08	2011fe	-11	12262(39)	186(2)	NV	1.18
2002bo	-6.3	14455(156)	220(12)	HV	1.08	2011fe	-10	11879(38)	183(2)	NV	1.18
2002bo	-5.4	14172(154)	216(11)	HV	1.08	2011fe	-9	11526(50)	175(2)	NV	1.18
2002bo	-4.4	13939(152)	216(11)	HV	1.08	2011fe	-8	11287(49)	175(2)	NV	1.18
2002bo	-3.4	13681(151)	213(11)	HV	1.08	2011fe	-7	11067(55)	165(2)	NV	1.18
2002bo	-2.5	13433(148)	211(11)	HV	1.08	2011fe	-6	10907(54)	162(2)	NV	1.18
2002bo	-1.5	13217(145)	208(11)	HV	1.08	2011fe	-5	10815(47)	160(2)	NV	1.18

Continued on next page

Table 2 continued

SN	Phase (days)	V^{Si6} (km/s)	γ^{Si6} (Å)	subtype	Δm_{15} (mag)	SN	Phase (days)	V^{Si6} (km/s)	γ^{Si6} (Å)	subtype	Δm_{15} (mag)
2002cd	-3.7	15201(205)	176(9)	unclear	0.794	2011fe	-1	10386(64)	150(2)	NV	1.18
2002cd	0.3	14979(193)	165(9)	unclear	0.794	2011fe	0	10296(85)	148(3)	NV	1.18
2002er	-3.9	11740(131)	159(8)	NV	1.23	2011fe	1	10220(146)	147(8)	NV	1.18
2002er	0.1	11491(129)	167(9)	NV	1.23	2011fe	3	10089(156)	145(8)	NV	1.18
2002he	-3.3	12641(141)	169(9)	HV	1.494	2011fe	4	10066(167)	147(8)	NV	1.18
2002he	0.2	12155(134)	167(9)	HV	1.494	2011fe	-5	10815(47)	159(2)	NV	1.18
2003W	-3.4	14445(236)	226(7)	unclear	1.113	2011fe	0	10296(85)	149(3)	NV	1.18
2003W	-0.3	14133(157)	214(4)	unclear	1.113	2012fr	-12.5	15500(160)	283(2)	99aa	0.8
2003cg	-4.1	11225(135)	145(8)	NV	1.22	2012fr	-11.5	14572(39)	252(2)	99aa	0.8
2003cg	-0.2	10851(127)	141(8)	NV	1.22	2012fr	-6.4	13131(55)	203(2)	99aa	0.8
2003du	-14.1	13210(71)	200(11)	NV	1.07	2012fr	-2.4	12905(147)	183(7)	99aa	0.8
2003du	-12.1	12103(89)	195(4)	NV	1.07	2012fr	-1.3	12969(165)	181(7)	99aa	0.8
2003du	-8.1	10973(45)	162(2)	NV	1.07	2012fr	-0.4	12936(169)	178(7)	99aa	0.8
2003du	-7.1	10632(56)	157(2)	NV	1.07	2012fr	0	13195(175)	167(6)	99aa	0.8
2003du	-6.1	10773(141)	163(9)	NV	1.07	2012fr	2	13338(194)	156(6)	99aa	0.8
2003du	-5.1	10413(81)	147(2)	NV	1.07	2012fr	3	12996(137)	150(3)	99aa	0.8
2003du	-4.1	10474(131)	155(8)	NV	1.07	2014J	-11	14267(155)	186(10)	HV	1.022
2003du	-3.1	10195(134)	145(8)	NV	1.07	2014J	-9	13619(150)	183(10)	HV	1.022
2003du	-2.1	10280(117)	143(8)	NV	1.07	2014J	-7	12856(137)	177(9)	HV	1.022
2003du	-1.1	10250(117)	143(8)	NV	1.07	2014J	-5	12642(135)	167(9)	HV	1.022
2003du	-0.1	10133(119)	137(7)	NV	1.07	2014J	-3	12309(130)	162(9)	HV	1.022
2003du	0.9	10262(147)	138(8)	NV	1.07	2014J	-2	11910(126)	160(9)	HV	1.022
2003du	1.9	9789(116)	138(7)	NV	1.07	2014J	0	12012(128)	155(8)	HV	1.022
2003du	2.9	10052(130)	135(7)	NV	1.07	2014J	3	11930(129)	147(8)	HV	1.022
2003du	4.9	10115(129)	132(7)	NV	1.07	2014J	-5	12642(135)	166(9)	HV	1.022
2003du	5.9	10187(160)	137(8)	NV	1.07	2014J	0	12012(128)	155(8)	HV	1.022
2003du	-4.1	10474(131)	155(8)	NV	1.07						

Note: ' V^{Si6} ' and ' γ^{Si6} ' represent the velocity and FWHM of Si II $\lambda 6355$, respectively. ' Δm_{15} ' represents the B-band decline rate;

Table 3: The absorption depths and FWHMs of Si II $\lambda 5972$

SN	Phase (days)	A^{Si5} (km/s)	γ^{Si5} (Å)	Δm_{15} (mag)	SN	Phase (days)	A^{Si5} (km/s)	γ^{Si5} (Å)	Δm_{15} (mag)
1981B	0	0.1728(0.0046)	181(10)	0.91	2004as	-0.1	0.1447(0.0046)	182(10)	1.111
1986G	0	0.3655(0.0091)	161(9)	1.65	2004at	0.2	0.1282(0.0042)	88(6)	1.091

Continued on next page

Table 3 continued

SN	Phase (days)	A^{Si5} (km/s)	γ^{Si5} (Å)	Δm_{15} (mag)	SN	Phase (days)	A^{Si5} (km/s)	γ^{Si5} (Å)	Δm_{15} (mag)
1989B	-1	0.1739(0.005)	174(9)	1.35	2004gs	-0.3	0.3601(0.0158)	154(8)	1.775
1992A	0	0.2353(0.0093)	162(9)	1.41	2005A	0.6	0.0996(0.0029)	161(9)	1.222
1994ae	0	0.123(0.0029)	137(7)	0.96	2005M	-0.1	0.1396(0.0037)	168(9)	0.827
1995E	-0.2	0.2178(0.007)	160(9)	1.16	2005cf	0.3	0.1498(0.0039)	86(7)	1.1
1996X	-0.1	0.1315(0.0056)	138(6)	1.26	2005eq	0.4	0.0989(0.0024)	128(7)	0.882
1996ai	0.1	0.098(0.0033)	134(7)	1	2005ke	-0.3	0.3942(0.0099)	158(8)	1.762
1997bp	-0.2	0.0797(0.0019)	119(6)	1.08	2005na	0.5	0.1094(0.0039)	136(7)	1.239
1997dt	0.2	0.0957(0.0023)	106(6)	1.04	2006N	0.7	0.1608(0.0042)	138(7)	1.57
1998aq	-0.2	0.1075(0.0028)	126(7)	1.11	2006S	0.3	0.0512(0.0015)	135(7)	0.9
1998bp	-2.9	0.4051(0.012)	118(6)	1.83	2006ax	0.2	0.1268(0.0022)	143(7)	1.016
1998bp	-1.9	0.4027(0.0106)	120(7)	1.83	2006bt	-0.1	0.3367(0.0127)	176(9)	0.877
1998bp	-0.9	0.4091(0.0107)	122(7)	1.83	2006cj	-0.2	0.1785(0.0207)	142(9)	0.81
1998bp	0.1	0.407(0.0099)	121(7)	1.83	2006gt	-0.1	0.4231(0.029)	121(3)	1.66
1998bp	1	0.4015(0.01)	125(7)	1.83	2006sr	-1	0.1795(0.0051)	158(8)	1.39
1998de	-0.3	0.4557(0.0184)	152(8)	1.93	2007A	0.4	0.1224(0.0038)	128(6)	0.946
1998dh	-0.5	0.1947(0.0048)	130(7)	1.227	2007F	-0.9	0.1101(0.0042)	136(7)	1.03
1998dx	-0.7	0.1943(0.0164)	133(5)	1.55	2007S	-0.8	0.0664(0.0017)	145(8)	1.096
1998es	-0.5	0.0803(0.0019)	137(7)	0.978	2007af	0.3	0.1989(0.0059)	129(7)	1.2
1999aa	-11.4	0.1216(0.0032)	233(11)	0.94	2007bc	0.4	0.3042(0.0084)	153(8)	1.349
1999aa	-10	0.1232(0.0022)	286(15)	0.94	2007ci	-8.2	0.3839(0.0175)	174(5)	1.744
1999aa	-9.1	0.1274(0.0019)	257(13)	0.94	2007ci	-7.2	0.423(0.0167)	182(10)	1.744
1999aa	-8.1	0.1197(0.002)	238(12)	0.94	2007ci	-6.2	0.3698(0.0133)	182(10)	1.744
1999aa	-7.2	0.1127(0.0022)	226(12)	0.94	2007ci	-5.2	0.3574(0.0101)	170(9)	1.744
1999aa	-6.1	0.1132(0.0023)	199(11)	0.94	2007ci	-4.2	0.324(0.0087)	158(8)	1.744
1999aa	-5.1	0.0902(0.0022)	168(9)	0.94	2007ci	-2.2	0.3165(0.0092)	162(9)	1.744
1999aa	-4.1	0.0766(0.0017)	150(8)	0.94	2007ci	-1.2	0.3123(0.0098)	158(9)	1.744
1999aa	-3.1	0.0754(0.0017)	145(8)	0.94	2007co	-0.2	0.1326(0.0049)	135(7)	1.04
1999aa	-2.1	0.0727(0.0017)	137(7)	0.94	2007hj	-2.6	0.4286(0.0115)	152(8)	1.953
1999aa	-0.1	0.0837(0.002)	132(7)	0.94	2007hj	-1.5	0.4073(0.0104)	145(8)	1.953
1999ac	-1	0.1252(0.0023)	161(4)	1.182	2007hj	-0.6	0.4193(0.011)	146(8)	1.953
1999cc	-0.2	0.2388(0.0096)	143(8)	1.46	2007hj	1.4	0.3745(0.0103)	141(8)	1.953
1999cl	0.7	0.1609(0.0037)	171(9)	1.144	2007hj	2.4	0.4017(0.0114)	141(8)	1.953
1999dq	0.5	0.0832(0.0019)	173(9)	0.961	2007hj	3.5	0.3799(0.0091)	144(8)	1.953
1999ee	-0.4	0.1068(0.0025)	189(10)	0.96	2007hj	4.4	0.3766(0.0094)	137(7)	1.953
1999gp	0	0.0324(0.0017)	143(11)	0.908	2008Q	-0.3	0.1777(0.0087)	90(9)	1.25
2000cx	0.2	0.1073(0.0027)	138(7)	0.99	2008ar	-0.7	0.1425(0.005)	90(5)	1.078

Continued on next page

Table 3 continued

SN	Phase (days)	A^{Si5} (km/s)	γ^{Si5} (Å)	Δm_{15} (mag)	SN	Phase (days)	A^{Si5} (km/s)	γ^{Si5} (Å)	Δm_{15} (mag)
2000dk	0.4	0.3554(0.0089)	135(7)	1.718	2008bf	0.7	0.0917(0.0027)	116(6)	1.029
2001cp	0.9	0.0719(0.0023)	91(5)	0.915	2011fe	-15	0.2418(0.0032)	192(4)	1.18
2001da	0	0.19(0.0052)	156(8)	1.23	2011fe	-14	0.2937(0.0035)	187(6)	1.18
2001eh	-0.1	0.0573(0.0036)	131(17)	0.811	2011fe	-13	0.2841(0.0034)	179(4)	1.18
2001ep	-0.2	0.2792(0.0073)	165(9)	1.356	2011fe	-12	0.2929(0.0023)	185(4)	1.18
2001fe	0.3	0.0947(0.0022)	123(7)	1.03	2011fe	-11	0.2792(0.0031)	181(4)	1.18
2002cd	0.3	0.055(0.0018)	105(6)	0.794	2011fe	-10	0.266(0.003)	182(4)	1.18
2002cr	0.7	0.2311(0.0067)	129(7)	1.229	2011fe	-9	0.2447(0.0037)	175(9)	1.18
2002er	0.1	0.1492(0.0039)	123(7)	1.23	2011fe	-8	0.2386(0.0058)	150(8)	1.18
2002he	-8.3	0.2962(0.017)	163(5)	1.494	2011fe	-7	0.216(0.0037)	165(9)	1.18
2002he	-6.2	0.2317(0.0082)	148(8)	1.494	2011fe	-6	0.2104(0.0036)	161(9)	1.18
2002he	-3.3	0.1927(0.0049)	138(7)	1.494	2011fe	-5	0.2124(0.0032)	159(8)	1.18
2002he	-1.2	0.1668(0.0048)	122(7)	1.494	2011fe	-1	0.176(0.0041)	135(6)	1.18
2002he	0.2	0.1921(0.0048)	140(8)	1.494	2011fe	0	0.1768(0.0053)	134(7)	1.18
2002he	3.2	0.2214(0.0054)	159(8)	1.494	2011fe	1	0.1736(0.0068)	131(7)	1.18
2002he	5.7	0.2155(0.0104)	108(7)	1.494	2011fe	3	0.1674(0.0073)	143(8)	1.18
2002kf	0.8	0.1924(0.0063)	133(7)	1.2	2011fe	4	0.1916(0.0093)	147(8)	1.18
2003W	-0.3	0.0607(0.002)	174(7)	1.113	2012fr	-12.5	0.0908(0.002)	192(9)	0.8
2003cg	-0.2	0.1701(0.0048)	102(6)	1.22	2012fr	-11.5	0.0801(0.0012)	178(9)	0.8
2003ch	-0.2	0.1703(0.0106)	120(4)	1.22	2012fr	-6.4	0.0797(0.002)	103(4)	0.8
2003cq	0.1	0.2289(0.0294)	162(8)	1.26	2012fr	-2.4	0.0664(0.0018)	110(6)	0.8
2003du	-0.1	0.0965(0.0027)	109(6)	1.07	2012fr	-1.3	0.0647(0.0021)	120(7)	0.8
2003it	-0.2	0.1589(0.0039)	123(4)	1.36	2012fr	-0.4	0.0777(0.0027)	126(7)	0.8
2003iv	0.1	0.253(0.0135)	121(4)	1.65	2014J	0	0.1131(0.0026)	127(7)	1.022

Note: ' A^{Si5} ' represents the absorption depth of Si II $\lambda 5972$, ' γ^{Si5} ' represents the FWHM of Si II $\lambda 5972$.